

Muons tomography applied to geosciences and volcanology

J. Marteau^{a,*}, D. Gibert^b, N. Lesparre^b, F. Nicollin^c, P. Noli^d, F. Giacoppo^e

^a*Institut de Physique Nucléaire de Lyon (UMR CNRS-IN2P3 5822), Université Lyon 1, Lyon, France.*

^b*Institut de Physique du Globe de Paris (UMR CNRS 7154), Sorbonne Paris Cité, Paris, France.*

^c*Géosciences Rennes (CNRS UMR 6118), Université Rennes 1, Bât. 15 Campus de Beaulieu, 35042 Rennes cedex, France.*

^d*Università degli studi di Napoli Federico II & INFN sez. Napoli, Italy.*

^e*Laboratory for High Energy Physics, University of Bern, SidlerStrasse 5, CH-3012 Bern, Switzerland.*

Abstract

Imaging the inner part of large geological targets is an important issue in geosciences with various applications. Different approaches already exist (e.g. gravimetry, electrical tomography) that give access to a wide range of informations but with identified limitations or drawbacks (e.g. intrinsic ambiguity of the inverse problem, time consuming deployment of sensors over large distances). Here we present an alternative and complementary tomography method based on the measurement of the cosmic muons flux attenuation through the geological structures. We detail the basics of this muon tomography with a special emphasis on the photo-active detectors.

Keywords: cosmic rays, muon, volcano, tomography, telescope

PACS: 14.60.-z, 95.55.Vj, 91.40.-k, 93.85.-q

1. Introduction and motivations

Monitoring natural events such as earthquakes, volcanic eruptions, landslides and tsunamis has immense importance, both scientific and societal. The interest of volcano radiography arose in the last decades in Japan [1–4], which has a large volcanic and seismic activity, like other places in the world such as Italy and Iceland in Europe or the Antilles belt in the Atlantic ocean. Because of the possible vicinity of populated areas, volcanoes require careful monitoring of their activity and precise modelling of their geophysical evolution.

Consider for instance Lesser Antilles, a subduction volcanic arc with a dozen of active volcanoes located in populated areas. The volcanoes of Martinique (La Montagne Pelée), Guadeloupe (La Soufrière), and Montserrat (The Soufrière Hills) presented an eruptive activity since the beginning of the 20th century. It is therefore crucial to

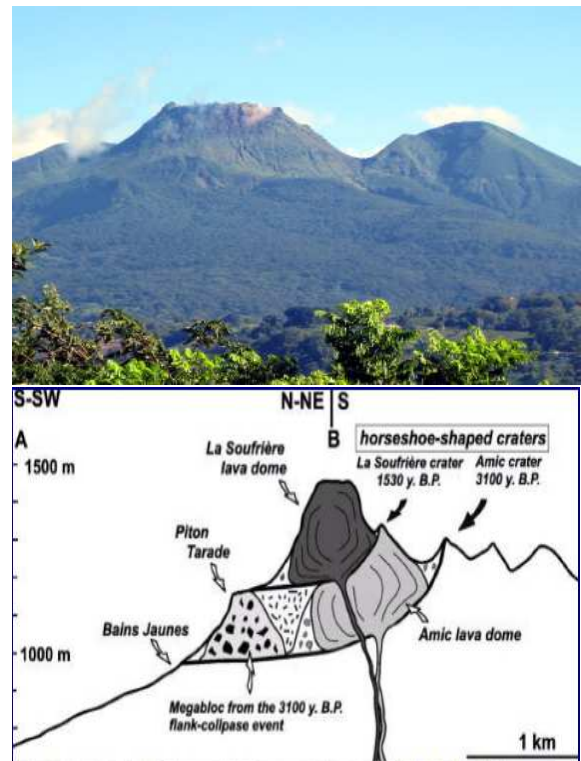


Figure 1: La Soufrière of Guadeloupe: picture and model.

*Corresponding author

Email address: marteau@ipnl.in2p3.fr (J. Marteau)

18 evaluate their eruptive evolution in the near future to and 55
19 quantify the associated risk for surrounding inhabitants. 56
20 Reaching these goals requires accurate imaging of the vol- 57
21 cano’s inner structure and quantitative estimates of the 58
22 related parameters (variations of volume, density, strain, 59
23 or pressure) associated with fluid transports (magma, gas, 60
24 or water) or physical and chemical evolution of the volcanic 61
25 materials. La Soufrière of Guadeloupe, an andesitic vol- 62
26 cano whose lava dome is about five hundred years old [5], 63
27 is particularly relevant since it presents a diversified num- 64
28 ber of hazards including phreatic eruption, flank collapse 65
29 and explosive magmatic eruption [6]. Its dome is very het- 66
30 erogeneous, with massive lava volumes embedded in more 67
31 or less hydrothermalized materials [7]. Given the constant 68
32 erosion of the volcano due to the tropical intensive rain 69
33 activity, the evolution of such a lacunary structure may be 70
34 rapid, with formation of cavities, that may be filled with
35 pressurized and likely very acid fluids, resulting in flank
36 destabilization. On top of that present structural mod-
37 els show that the dome sits on a 15° N-S inclined plane,
38 leading to an overall very unstable structure (Fig.1). This
39 particular example shows that a precise knowledge of the
40 dome’s internal structure is a key issue for the global mod-
41 elling and understanding of the volcanoes. For this reason,
42 La Soufrière has been chosen as priority target for muon
43 imaging [8], which constitutes one of the most promising
44 tools to obtain direct information on the density distribu-
45 tion inside geological objects.

46 2. Tomography basics

47 The interest of muon tomography for Earth Sciences
48 purposes soon arose after the discovery of cosmic rays
49 and of the muon. The cross-section of that particle at
50 those typical energies makes it a perfect probe since it is
51 able to cross hundredths of meters of rock with an attenu-
52 ation related to the amount of matter along its trajectory
53 [9]. Since it is a charged particle, its detection is quite 71
54 straightforward. The first studies relevant to tomography 72

in geosciences, were motivated by the need to characterise
the geological burden overlying underground structures, in
particular laboratories hosting large particles experiments
aimed at detecting rare events in a silent environment (the
so-called “cosmic silence” [10]). This type of “underground
tomography” is pursued nowadays in the applications of
long-term storage where detailed knowledge is required on
the geological environment (nature and borders of vari-
ous layers) and for mining geophysics. Applications other
than those directly related to underground physics require
smaller, modular, autonomous detectors movable on the
field and able to reject efficiently the background. The
pioneering archaeological investigations performed in the
Egyptian Chephren pyramid by Alvarez et al. in the seven-
ties [11], looking for some hidden room inside the pyramid,
reveal the feasibility of the method.

A muon radiography uses the same basic principles
than a standard medical radiography: measuring the at-
tenuation of a beam (cosmic muons versus X-rays) when
crossing matter (rock vs human flesh) with a sensitive
device. A detailed discussion of all parameters is given
in [12]. The measurement gives access to the opacity ϱ of
the geological structures by comparing the muons flux Φ
after crossing the target to the incident open sky flux, Φ_0 .
Various models give analytical expressions of the muon
flux from the two-body decays of pions and kaons and
assuming a primary proton flux spectrum roughly follow-
ing a power law $\approx E_p^{-2.7}$ [13–15]. The opacity is con-
verted to density ρ by inverting the integral equation :
 $\varrho(\text{kg.m}^{-2}) \equiv \int_L \rho(\xi) d\xi$, L denoting particles trajectory with
local coordinate ξ . The muons energy loss (and potential
absorption) on their way through rock accounts for the
standard bremsstrahlung, nuclear interactions, and e^-e^+
pair production physical processes, taken as :

$$-\frac{dE}{d\varrho}(\text{MeV g}^{-1} \text{cm}^2) = a(E) + b(E)E, \quad (1)$$

where the functions a and b depend on the crossed mater-
ial properties [16]. The flux of muons emerging from the

73 target is the integral of Φ over the energy, ranging from 94
 74 $E_{\min}(\varrho)$, the minimum initial energy necessary to cross 95
 given opacity ϱ , to infinite (Fig.2). This flux is influenced 96

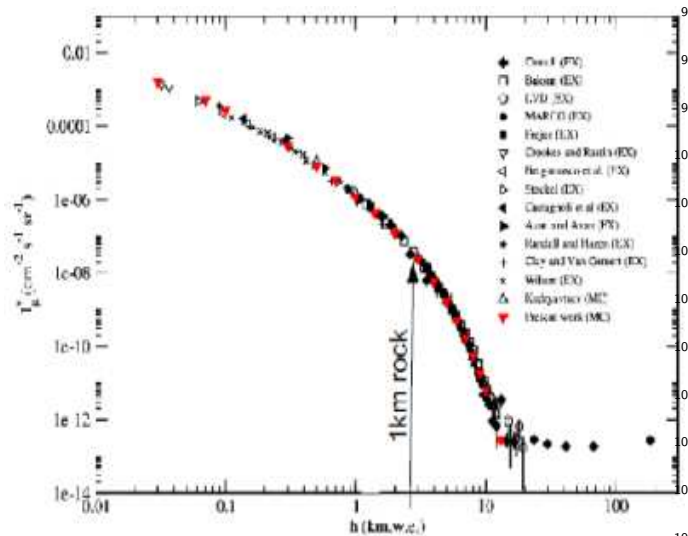


Figure 2: Integrated flux computed as a function of the standard 109
 rock thickness L in meters-water-equivalent (m.w.e.) compared to 110
 experimental points.

75
 76 by various environmental parameters such as altitude, geo- 112
 77 magnetic cut-off, solar modulation, atmospheric variations 113
 78 to be accounted for in the simulation models. Finally the 114
 79 number of detected muons is the convolution of the muons 115
 80 flux crossing the target, the data taking duration and the 116
 81 telescope acceptance, which is the key experimental para- 117
 82 meter that one may evaluate from the simulation and/or 118
 83 from the data themselves.

84 3. Photo-active detectors for tomography

85 3.1. The DIAPHANE project

86 DIAPHANE is the first european project of tomography 123
 87 applied to volcanology. It started in 2008 with a collabora- 124
 88 tion between three French institutes : IPG Paris, IPN 125
 89 Lyon and Géosciences Rennes to promote muon tomo- 126
 90 graphy in the French Earth Science and Particle Physics 127
 91 communities [8]. The first objectives of the project were to 128
 92 make technological choices for the muon telescopes and to 129
 93 define a design suitable for the difficult field conditions 130

encountered on the Lesser Antilles volcanoes. The de-
 97 tector’s design : plastic scintillator, optical fibres, pixelized
 98 photomultipliers and triggerless, smart, Ethernet-capable
 99 readout electronics, is based on the state-of-the-art opto-
 100 electronics technology, known for its robustness and stabil-
 101 ity in extreme working conditions. Modularity and limits
 102 in weight are also imposed by transportation constraints,
 103 some positions on the flank of the volcanoes being access-
 104 ible only by helicopter. A standard detector (or “tele-
 105 scope”) comprises 3 independant XY detection planes with
 106 autonomous and low power consumption readout system
 107 recording and timestamping their own hits in auto-trigger
 108 mode. The event-building is performed quasi on-line, via
 looking for time coincidences between hits passing the vari-
 109 ous trigger cuts. Data are transferred continuously via
 Ethernet wifi and are directly accessible remotely. No shift
 110 on-site are needed (concept of the unmanned sensors). The
 111 detector is powered through solar panels. Weight, power
 112 consumption, robustness and costs have been optimized
 113 to the best achievable compromises for that type of field
 114 operating detector [17].

Detection matrices. Two layers (X & Y) scintillator bars
 115 are glued between 1.5 mm thick anodised aluminium plates.
 116 The scintillator bars were provided by Fermilab with a
 117 rectangular cross-section of 5×1 cm² and are co-extruded
 118 with a TiO₂ reflective coating and a 1.5 mm diameter
 119 central hole to host an optical fibre [18]. Two different
 120 fibres are used to optimize the emission-absorption spectra
 121 matching and decrease the attenuation length : wavelength
 122 shifting (WLS) fibre (Bicron BCF 91A MC) glued with
 123 standard optical cement (Bicron BC-600) in the bar and,
 124 through a custom PEEK optical connector, a clear fibre
 125 (Bicron BCF-98 MC) down to the photosensor. Three
 126 matrices are used in coincidence in a complete telescope.
 127 The total aperture angle and the angular resolution of
 128 the telescope may be adjusted by changing the distance
 129

131 between the matrices.

132 *Photodetectors.* Hamamatsu 64 channels multi-anode pho-
133 tomultipliers are used baseline photosensors (H8804-mod5
134 and its upgraded version H8804-200mod). These PMTs
135 are robust and do not exhibit any temperature/humidity
136 dependance. Their gains and pedestals are monitored reg-
137 ularly and are stable within a few percents. The present
138 design also foresees optional upgrade with Hamamatsu
139 MPPC (S10362-11-050C) directly connected onto the op-
140 tical plugs of the scintillator bars w/o the clear fibres.
141 The MPPCs have very attractive performances in terms
142 of single photon sensitivity and photon resolution power,
143 which are key features to improve the muon detection ef-
144 ficiency. Nevertheless their dark count rates and thermal
145 fluctuations are a concern and require careful commission-
146 ing. Dedicated electronics, adapted from the PMT's one,
147 is presently under tests.

148 *Readout system.* The global data acquisition system is
149 built as a network of “smart sensors” [19, 20]. The PMT
150 data are collected by two multichannel front-end chips,
151 then digitized and pre-processed by an Ethernet Control-
152 ler Module (hosting a 32-bit RISC CPU with a Linux 2.4
153 OS, a FPGA and a FIFO) plugged on a Controller Mother
154 Board (including a fast ADC, a HV module and a clock
155 decoding system). The same type architecture is also valid
156 for the MPPC option where only the front-end stage has
157 to be adapted. The distributed client/server software is
158 based on the CORBA standard. Since the telescope is
159 running in triggerless mode, event timestamp accuracy is
160 a critical issue. A clock broadcasting system synchronizes
161 all sensors with a common clock unit regulated by GPS.

162 *Mechanical structure.* The frame of the telescope is built
163 with slotted and anodised aluminium profiles. The detec-
164 tion matrices and R/O system fit in a single box made with
165 4 profiles and two 1 mm thick aluminium plates. Tight-
166 ness against water and light is obtained with a seal ap-
167 plied between the aluminium plates and the profiles. Four

168 connectors complying with the IP67 norm are used to en-
169 sure power supply and data transfer, and a valve equipped
170 with a Gore Tex membrane allows evacuation of water va-
171 pour without letting liquid water to penetrate into the box.
172 The supporting structure of the telescope is made with the
173 same type of profiles, the full structure being articulated
174 to change the inclination of the matrices. Pictures of the
telescope are shown in Fig.3.



Figure 3: Left: detection plane with 16×16 scintillator bars, connected via optical fibres to the PMT+R/O system. Right: a3-planes detector installed on La Soufrière (Ravine Sud).

3.2. First results and comparisons with other methods

As stated above, the acceptance of the telescope is a key parameter since the goal of the project is to assign an opacity and therefore a density to the target from an absolute measurement of flux. Many corrections may be inferred to the theoretical acceptance deduced from solid angles calculations. The experimental inefficiencies are corrected either directly from the light yield measurement or indirectly from the overall data sets themselves. Details on the methods may be found in Ref.[12, 21]. Typical acceptance curves and corrected open sky muons flux (showing the expected symmetry) are shown in Fig.4.

Three DIAPHANE telescopes have been built and have been recording data on the field. The first one was put in the Mont-Terri underground laboratory (Switzerland), located in an anticline formed with layers of Opalinus clay and limestones with densities $\rho_{\text{clay}} = 2.4$ and $\rho_{\text{lime}} = 2.7$ [22]. This place was chosen to fully commission in-situ a muon telescope and constrain detector performance, data

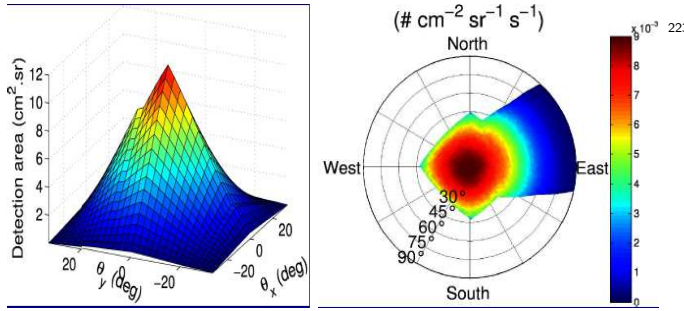


Figure 4: Left: acceptance function of a 16×16 3-planes detector before correction. Right: corrected open sky muons flux.

analysis and simulations models since the geological layers and topography are well known. This telescope is still taking data and is deployed in various places of the galaxy to sample the geological layers and make redundant measurements.

The second telescope has been deployed on the Etna volcano for a short trial period during summer 2010 and was able to see within a few days the profile of the volcano. The scale of this volcano implies that, at the current state of the art, only a small portion of its edifice can be investigated through muon imaging. Further campaigns are planned on the Etna following preliminary studies detailed in [12].

The third telescope has been installed on La Soufrière of Guadeloupe, one of the volcanoes with hardest environmental conditions. The geophysics case of this volcano was discussed in the previous sections. Two sites have been already explored, roughly at 90° of each other (“Ravine Sud”, accessible by car and “Roche Fendue” only accessible by helicopter). These two orthogonal views show not only a very good compatibility with each other but also with other measurements carried out with different methods on the same place (gravimetry and electrical tomography). Fig.5 shows the large density variations observed in the inner structure. Preliminary analysis indicates presence of large low density volumes within the cone, also seen in electrical tomographic data (highly conductive zones being inferred either to hydrothermally washed zones or to

acid zones), and reveals the existence of large hydrothermal channels to be accurately monitored. The DIAPHANE

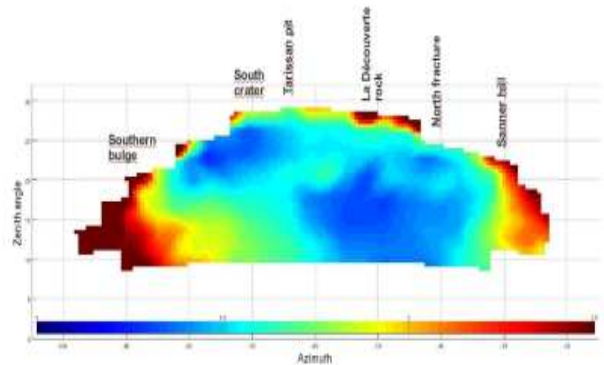


Figure 5: Density profile obtained at the Roche Fendue site.

project has very rich and intense perspectives with the exploration of other fields of view and at a short-term scale the deployment of a network of telescopes (with larger acceptance) running in parallel to perform real-time 3D tomography of the volcano and sample some particularly sensitive zones (like recently opened faults) that may evolve quickly in time.

3.3. The MURAY project

The MU-RAY project [23] aims at the construction of muon telescopes with angular resolution comparable with that obtainable with emulsions, but with real-time data acquisition and larger sensitive area. The telescopes are required to be able to work in harsh environment imposing a modular structure, each module being light enough to be easily transported by hand. Further requirements are mechanical robustness and easy installation. Power budget must fit a small solar panel system’s capability. Good time resolution can improve background suppression by measuring the muon time of flight.

Scintillator features. A telescope prototype is built in Naples University laboratory and it consists of three $1 \times 1m^2 XY$ stations (Fig.6). The third station will be used to study possible backgrounds, as the one induced by cosmic-ray showers. Each station is made by two planes disposed in

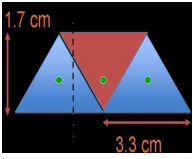


Figure 6: Left: triangular shape of the scintillator bars used in the MURAY project. Right: a3-planes detector in the lab.

orthogonal way. Each plane is composed by two adjacent modules made by 32 triangular plastic scintillator strips. Scintillator bars are produced by extrusion process at Fermilab, for D0 [24] and Minerva [25] experiments, in pieces as long as 6m, with a hole along the center. The core (Dow Styron 663W) is doped with blue-emitting fluorescent compounds (PPO 1% and POPOP 0.03%). The surface has a co-extruded TiO₂ coating (0.25mm thick) to increase internal reflectivity and to shield from environment light. The use of isosceles triangular shape allows the construction of very compact, crack-free planes. Moreover, the measurement of the light output produced by two adjacent strips enables the determination of the particle crossing distance between two contiguous fibers, improving the spatial resolution. The triangular bars are glued to each other and over two 2mm thick fibreglass plates, creating a very solid module. Light from scintillator is collected by 1mm diameter WLS fibre BICRON BCF92, glued inside the bar to maximize light collection efficiency. Fibres are mirrored at one end using the Al sputtering facility of the Frascati INFN laboratory [26].

Photodetectors and electronics. The light is readout by silicon photomultipliers (SiPM) [27, 28] which offer several advantages. Their robustness is mandatory for the environmental conditions; their very low power consumption (less than 1mW per channel) is relevant due to limited power budget. One of main SiPM drawbacks is the gain-temperature dependence that affects the detector performance. For this reason the SiPMs' temperature will be con-

trolled using Peltier cells. In order to optimize the power consumption, we decided to group together 32 die SiPMs in a single connector (PCB). The fibres are glued to a custom 32-channel optical connector, which will be fixed to the module chassis and mechanically coupled with the PCB. One side of the Peltier cells is thermally in contact with the back side of the PCB while plastic guarantees a good thermal insulation with respect to the environmental temperature. A rubber O-ring around the sensitive area is used to ensure light and air tightness. Two temperature sensors are located on the PCB for the Peltier cells control circuit. The SiPM front-end electronics readout is based on SiPM Read-Out Chip (SPIROC) ASIC developed by OMEGA group (LAL, CNRS-IN2P3 [29]).

Geophysics case. Today around 600,000 people are living at the base and along the slopes of the Vesuvius volcano, in a so-called "red" area which has been classified at the highest volcanic risk in Europe. Mt. Vesuvius is therefore among the most studied volcanoes in the world. The knowledge of the inner structure of the volcano edifice and subsoil structure is of the greatest importance to build realistic scenarios of the next eruption through accurate simulations (magma uprising mechanism and eruption). Even if the Vesuvius has been thoroughly investigated using the traditional geophysical methods (gravimetric, seismological, electromagnetic), muon radiography may help by improving the resolution of the cone inner structure by one order of magnitude.

4. Other techniques : gaseous detectors and nuclear emulsions

4.1. Gaseous detectors

Since there is not an unique way to detect muons, various projects arose recently using gaseous detectors: glass RPC for the TOMUVOL project (radiography of the Puy-de-Dôme, Clermont-Ferrand, France) and gas TPC for the T2DM2 project (hydrogeology of the karst complex around

314 the LSBB, Rustrel, France). Those projects have taken
 315 their first data this year and interesting results are awaited
 316 soon.

317 4.2. Probing matter with emulsions

318 Nuclear emulsion particle detectors feature incompar-
 319 able high spatial and angular resolution ($< 1 \mu m$ and a
 320 few $mrad$, respectively) in the measurement of ionizing
 321 particles tracks. With the advent of fast electronic detect-
 322 ors, the emulsion technique has experienced a period of
 323 decline up to 20 years ago since when impressive progress
 324 in the high-speed automated scanning and industrial pro-
 325 duction have determined a new boost in the application
 326 of this technique in high-energy physics experiments. A
 327 nuclear emulsion is essentially a photographic plate where
 328 silver halide crystals with a typical size of $0.2 \mu m$ are ho-
 329 mogeneously dispersed in a gelatin matrix of about $50 \mu m$
 330 thickness. When such an emulsion is exposed to ionizing
 331 radiation or light, clusters of silver atoms are produced.
 332 These form latent image centres that became visible un-
 333 der an optical microscope when they are reduced to metal-
 334 lic silver filaments (grains) through a chemical developing
 335 process. A typical emulsion film produced industrially by
 336 FUJI Film Co., as a result of a joint R&D program with
 337 the OPERA Collaboration [30], consists of $\sim 10^{14}$ silver
 338 halide crystals. Each of them has a detection efficiency
 339 of 20% for minimum ionizing particle and a sensitivity of
 340 $30 \div 40$ halide grains per $100 \mu m$.

341 In addition to their spatial and angular resolution, tracker
 342 detectors based on nuclear emulsions are ideal for muon
 343 radiography for their data storage capability, portability
 344 and rather simple implementation in difficult environments
 345 such as, for examples, volcanoes. Moreover, nuclear emul-
 346 sion films do not need power supply and electronic front-
 347 end readout systems. The high spatial resolution of nuc-
 348 lear emulsion films was first exploited by Tanaka and his
 349 co-workers for the muon radiography of some volcanoes in
 350 Japan. In 2007 they performed a test measurement for

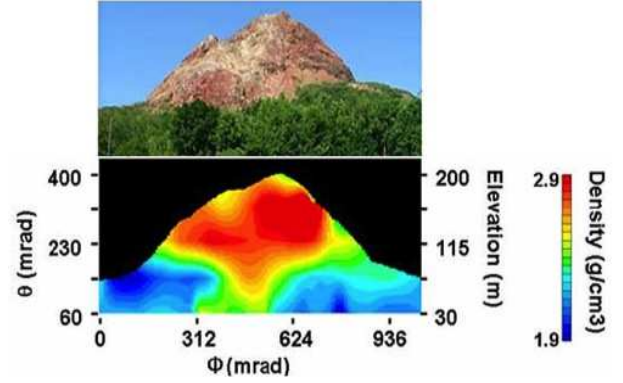


Figure 7: Top: view of the Showa-Shinzan lava dome. Bottom: average density distribution projected onto the detector's plane.

351 imaging the conduit of the Showa-Shinzan lava dome, on
 352 the east flank of Usu volcano by using quasi-horizontal
 353 cosmic-ray muons [31]. A muon detector consisting in a
 354 set of emulsion chambers with an area of 6000 cm^2 was
 355 exposed for three months. Fig. 7 shows the reconstructed
 356 average density of the dome summit. Recently the Labora-
 357 tory for High Energy Physics (LHEP) of the University
 358 of Bern has started an R&D program on nuclear emulsion
 359 detectors for muon radiography in the framework of the In-
 360 novative Nuclear Emulsion Technologies (INET) project,
 361 financed by the Switzerland-Russian Scientific and Tech-
 362 nological Cooperation Programme. A proof-of-principle
 363 test has been conceived in 2010 aimed at the detection
 364 of an existing (and known) mineral deposit inside a mine.
 365 Dedicated modular devices have been designed (see Fig. 8)
 366 and ten samples (emulsion film total area of 5000 cm^2)
 367 have been placed along the mine tunnel in order to meas-
 368 ure the underground muon flux at different locations. The
 369 combination of data from several modules would eventu-
 370 ally lead to a 3D image of the inner structure of the moun-
 371 tain.

Each emulsion chamber consists of two rectangular stain-
 372 less steel covers, containing four stacks of two emulsion
 373 doublets each. In order to reduce the effects of radiation
 374 coming from natural radioactivity, a lead plate is posi-
 375 tioned in the middle of each stack. The module mechanics
 376 is conceived to be tight to preserve the emulsion surface
 377

378 from light and humidity. After an exposure of 4.5 months⁴⁰⁶
379 the detector have been disassembled *in situ* inside a port-⁴⁰⁷
380 able dark room and the emulsion films developed and sent⁴⁰⁸
back to Bern. LHEP is one of the largest emulsion scan-⁴⁰⁹



Figure 8: Left: emulsion module hosting 16 emulsions. Middle: mod-⁴¹⁵
ule station during data taking. Right: reconstructed passing-through⁴¹⁶
tracks.

381
382 ning laboratories in the world where 5 state-of-the-art high⁴¹⁸
383 speed automatic microscopes are installed and routinely⁴¹⁹
384 operating for the OPERA experiment [32]. In addition, a⁴²⁰
385 new scanning station has been dedicated to muon radio-⁴²¹
386 graphy. The automated scanning system consists of a mi-⁴²²
387 croscope equipped with a computer-controlled motorized⁴²³
388 stage, a dedicated optical system and a CMOS camera⁴²⁴
389 [33]. For each field of view, several tomographic images⁴²⁵
390 of the emulsions are taken at equidistant depths by mov-⁴²⁶
391 ing the focal plane across the emulsion thickness (Z direc-⁴²⁷
392 tion). Images are grabbed and processed by a vision multi-
393 processor board, hosted in the control PC. The tracks are⁴²⁸
394 then reconstructed by combining grains from different lay-⁴²⁹
395 ers with a dedicated software program (see Fig. 8-(right)).⁴³⁰
396 For the extension of muon radiography measurements to⁴³¹
397 deeper structure as well as for reducing the exposure time,⁴³²
398 a larger emulsion surface would be needed. For this reason⁴³³
399 an upgrade of the current scanning system is foreseen, in⁴³⁴
400 order to reduce the scanning time. One promising solu-⁴³⁵
401 tion seems to be the use of high speed GPU (Graphic Pro-⁴³⁶
402 cessing Unit) to replace standard CPU for faster track re-⁴³⁷
403 construction. In the framework of INET, the LHEP group⁴³⁸
404 has set up a facility for “in-house” pouring and develop-⁴³⁹
405 ment of emulsion films. Several tests are ongoing with the

aim of producing suitable emulsion detectors (large area,
high sensitivity, low noise) for muon radiography and other
applications, especially in the medical field. Connections
with specialized companies providing emulsion gel have
been established for potential future large-scale produc-
tion.

412 5. Conclusions and perspectives

413 Muon tomography reaches a new era with mature, ro-
414 bust, adapted to harsh field conditions technologies de-
veloped and commissioned around the world. Volcanoes
are more and more targeted by muon tomographic ima-
ging since the alternative methods often reveal limited or
difficult to work out in their environments. The comple-
mentarity of the muon tomography with gravimetric or
electric tomography is emerging strongly since it offers
direct volume information with quasi straight lines of re-
sponses relatively easy to invert. The measurements are
also taken in a rather short timescale with a limited num-
ber of “shootings”. Promising real-time 3D tomographies
may offer to the community a powerful tool to monitor,
understand and better predict the behaviour of volcanoes,
with an obvious and crucial societal impact.

Acknowledgements

Authors from the DIAPHANE project warmly thank
K.Mahiouz, F.Mounier, P.Rolland, S.Vanzetto (opto-mechanics),
B.Carlus (informatics), S.Gardien, C.Girerd, B.Kergosien
(electronics) and colleagues from the Observatoire Vol-
canologique et Sismologique de Guadeloupe : A.Bosson,
F.Randriamora, T.Kitou, C.Lambert and V.Daniel. The
DIAPHANE project is financially supported by the IPGP
BQR grant, the DOMOSCAN ANR project, the CNRS/IN2P3
Astroparticles program, and the MD experiment of the
Mont Terri project funded by Swisstopo and CRIEPI part-
ners. The author would like to thank C.Carloganu and

440 P.Salin who contributed to the oral presentation. Emul-485
441 sions tomography project benefits from the strong support486
442 and expertise of the LHEP group. 487

[21] N. Lesparre, D. Gibert, J. Marteau, *Geophys. J. Int.*, in revision.
[22] P. Bossart, M. Thury, *Mont Terri Rock Laboratory Project, Programme 1996 to 2007 and Results*, Rep. Swiss Geological Survey
3, Wabern, Switzerland. 488

[23] <http://mu-ray.fisica.unina.it> 489

[24] P. Baringer, et al., *Nucl. Instr. and Meth. A* 469 (2001) 295. 490

[25] <http://minerva.fnal.gov> 491

[26] <http://www.lnf.infn.it/esperimenti/alice/emcal/sputtering/index.php> 492

[27] Z. Sadygov, Avalanche Detector, Russian Agency for Patents
and Trademarks, Patent No. RU 2102820 (1998). 493

[28] V. Golovin, Avalanche Photodetector, Russian Agency for Pat-
ents and Trademarks, Patent No. RU 2142175 (1999). 494

[29] <http://omega.in2p3.fr> 495

[30] T. Nakamura et al., *Nucl. Instr. & Meth. A* 556 (2006) 80. 496

[31] H. K. M. Tanaka et al. , *Geo. Res. Lett.* 34 (2007) L22311. 497

[32] R. Acquafredda et al., *JINST* 4 (2009) P04018. 498

[33] L. Arrabito et al., *JINST* 3 (2008) P04006. 499

443 References

444 [1] K. Nagamine, *J. Geogr.* 104 (1995) 998–1007.

445 [2] K. Nagamine, M. Iwasaki, K. Shimomura, K. Ishida, *Nucl. Instr.*
446 *and Meth. A* 356 (1995) 585–595. 493

447 [3] H.K.M. Tanaka, K. Nagamine, N. Kawamura, S.N. Nakamura, K.
448 Ishida, K. Shimomura, *Hyperfine Interact.* 138 (2001) 521–526. 494

449 [4] H.K.M. Tanaka, K. Nagamine, N. Kawamura, S.N. Nakamura, K.
450 Ishida, K. Shimomura, *Nucl. Instr. Meth. A* 507 (2003) 657–669. 495

451 [5] G. Boudon, J.-C. Komorowski, B. Villemant, M..P.
452 Semet, *J. Volcanol. Geotherm. Res.*, 178, 474-490, 500
453 doi:10.1016/j.jvolgeores.2008.03.006. 501

454 [6] J.-C. Komorowski, Y. Legendre, B. Caron, G. Boudon, *J. Vol-*
455 *canol. Geoth. Res.*, 178, 491-515.

456 [7] F. Nicollin, D. Gibert, F. Beauducel, G. Boudon, J.-C. Ko-
457 morowski, *Earth Planet. Sci. Lett.*, 244, 709–724.

458 [8] D. Gibert, F. Beauducel, Y. Déclais, N. Lesparre, J. Marteau,
459 F. Nicollin, A. Tarantola, *Earth Planets and Space* 62 (2010)
460 153–165.

461 [9] K. Nagamine, *Introductory Muon Science*, 208 pp, Cambridge
462 University Press, Cambridge UK, 2003.

463 [10] A. Zichichi, *Subnuclear physics: the first 50 years : highlights*
464 *from Erice to ELN*, 210pp, World Scientific Publishing, 2000.

465 [11] L.W. Alvarez, J.A. Anderson, F.E. Bedwei, J. Burkhard, A.
466 Fakhry, A. Girgis, A. Goneid, F. Hassan, D. Iverson, G. Lynch,
467 *Sci.* 167 (1970) 832–839.

468 [12] N. Lesparre, D. Gibert, J. Marteau, Y. Déclais, D. Carbone, E.
469 Galichet, *Geophys. J. Int.*, 183, 1348–1361.

470 [13] E.V. Bugaev, Yu D. Kotov, I.L. Rosental, *Cosmic muons and*
471 *neutrinos*, *Atomizdat*, Moscow.

472 [14] E.V. Bugaev, A. Misaki, V.A. Naumov, T.S. Sinegovskaya, S.I.
473 Sinegovsky, N. Takahashi, *Phys. Rev. D*, 58, 054001.

474 [15] T. Gaisser, *Cosmic rays and particle physics*, 279pp, Cambridge
475 University Press, 2000.

476 [16] <http://pdg.lbl.gov>

477 [17] N. Lesparre, J. Marteau, Y. Déclais, D. Gibert, B. Carlus, F.
478 Nicollin, B. Kergosien, *Nucl. Instr. Methods A*, in revision.

479 [18] A. Pla-Dalmau, A.D. Bross, K.L. Mellott, *Nucl. Instr. and*
480 *Meth. A* 466 (2001) 482–491.

481 [19] C. Girerd, S. Gardien, J. Burch, S. Katsanevas, J. Marteau,
482 *IEEE Nucl. Sci. Symposium and Nucl. Im. Conference* (2000)
483 7903.

484 [20] J. Marteau, *Nucl. Instr. and Meth. A* 617 (2010) 291–293.